



EFFECT OF SURFACE ROUGHNESS ON THE AERODYNAMIC AND AEROACOUSTIC PERFORMANCE OF THE DARRIEUS WIND TURBINE

J. Sarathkumar Sebastin, T J Ramkumar
Department of Aeronautical Engineering
Kalasalingam Academy of Research and Education
Sirivilliputhur, TamilNadu
sasisasi20720011@gmail.com

Abstract— The recent advancements in small wind turbines show an increased demand for the Darrieus wind turbine in the urban environment. The present work is devoted to the numerical analysis of the aeroacoustic sound emission from a straight bladed Darrieus wind turbine with NACA0018. Computations are performed at Reynolds number of 28,000 with a tip speed ratio of 0.4 using the unsteady Reynolds averaged Navier Stokes equations with Ffowcs Williams- Hawking's (FW-H) acoustic analogy. The FW-H method is based on a free field Green's function where the scheme uses a porous integration surface and implements an advanced time formulation. The study aims to obtain a numerical methodology to predict the effect of surface roughness on wind turbines' aerodynamic power and sound emission.

Keywords— *Darrieus wind turbine, Aeroacoustic, Aerodynamic power, Sound emission.*

I. INTRODUCTION

Wind energy has become essential due to ecologically viable power generation requirements. This vision is due to the adverse effects of combusting fossil fuels for power creation. Wind power usage leads to new wind turbines setting up near city zones. Hence, it is crucial to advance noise emission performance to the sound contamination in inhabited zones. The word noise defines the individual sensitivity of unnecessary sound waves in the human ear. The average human ear has a hearing range of 20 Hz to 20 kHz. In addition to conventional, sizeable horizontal axis wind turbines (HAWT), small wind turbines are considered an answer for wind power reaping, particularly on small scales in city zones. Inquiries in this space have concentrated on vertical axis wind turbines (VAWT). The VAWT doesn't need a yaw system. It can be applied in turbulent streams at low construction costs.

The utmost broadly known scheme of VAWTs is the Darrieus turbine [1], as shown in figure 1,2, established by the French engineer Darrieus in the twentieth century. Converting lift force is the supreme effective tactic to transform wind power into mechanical power [2]. In contrast, a representative drag-type method is a Savonius wind turbine. With a maximum power coefficient of 30%, the Savonius turbine does not apply to profitable wind power usage. Owing to wind turbines' growing energy and sound quality over the past decades, researching wind turbines' sound emissions is still a vital research area (Figure 3). In common, wind turbines have different sound sources. They can be distributed into two collections.

The first kind is mechanical sound, e.g. sound generated by auxiliary equipment such as gearboxes, generators, yaw drives, cooling fans, and hydraulics. The sound conduction path of mechanical sound is an airborne or structural sound. Another sound source is aerodynamic sound. Both sounds strongly depend on the rotor's geometry, airfoil profiles, and the adjacent flow situations. The sound conduction path of mechanical sound is an airborne or structural sound. Another sound source is aerodynamic sound. The sound conduction path of mechanical sound is an airborne or structural sound. Another sound source is aerodynamic sound. Both sounds strongly depend on the rotor's geometry, airfoil profiles, and the adjacent flow situations. The flow of air usually produces aerodynamic sound through the blades. Low-frequency sound is considered noise when revolving blades impede localised flow variations due to wind speed. The distinctive frequency range of low-frequency sound is around 10 Hz to 200 Hz. Low-frequency sound is primarily linked to the blade passing frequency and high harmonics. The airfoil profile of blades can create aerodynamic lift when exposed to the incident wind. This aerodynamic lift provides a moment along the blade axis, which allows the wind turbine's main shaft to rotate. Three-bladed VAWTs with straight blades are well suited for small-scale power production due to their blade design simplicity. In addition, VAWTs have certain benefits over HAWTs. Surface roughness is the one promising parameter to increase the aerodynamic power. But still, the studies need to analyse the sound Signals.

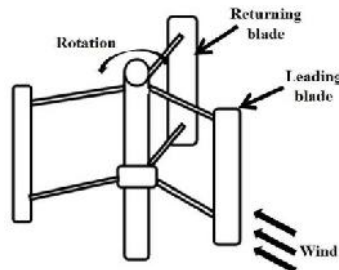


Figure.1. Three bladed Darrieus wind turbine

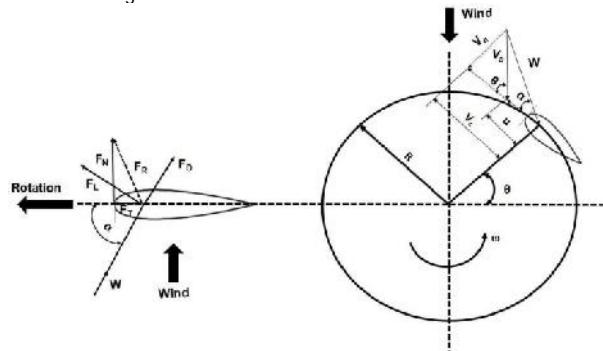


Figure.2. Loads and speed dissemination on Darrieus rotor airfoil

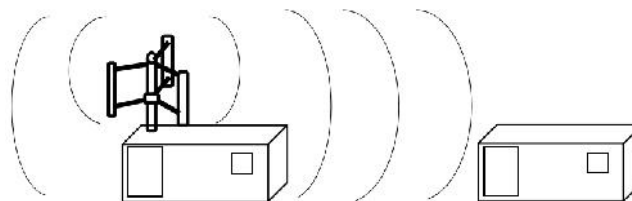


Figure 3. Wind turbine sound propagation

II. PROBLEM DEFINITION

In current years, experimental and numerical studies focusing on aerodynamic behaviour have been conducted in the field of VAWTs. Compared to traditional HAWTs, straight-bladed VAWTs are considered a viable solution in the municipal location. Therefore, it is essential to advance rotor performance and control noise discharge from the turbine blade to surrounding habitats. Based on the previous literature (Table 1), the main features for achieving high performance of the rotor are (i) Solidity [3-20]; (ii) the number of blades [21-24]; (iii) .blade profile [25-32]; (iv) .surface roughness [52-55]; (v) .Government Effect [33-41]; (vi).Pitch Control Strategy [42-51]; (vii) .Reynolds Number Effect [56-61]. Due to the recent progress of the CFD, the numerical investigation of the Darrieus wind turbines has attracted attention. The researchers found that the wind turbine's aeroacoustic characteristics could be calculated with reasonable accuracy using the CFD algorithm. Although these findings have revealed that the straight blade Darrieus wind turbine can be used to maximise aerodynamic performance, little consideration has been given to the aerodynamic noise issues. In this paper, attempts are being made to obtain a valid numerical method for finding a wind turbine's noise emission. Ffowcs Williams- Hawkins (FW-H) acoustic analogy is used to study sound emission. The study aims to analyse the effect of surface roughness on the darrieus turbine. Weber has experimentally and numerically investigated the Darrieus wind turbine with three blades. It is hoped that the current work will lead to more research in the aeroacoustics of the Darrieus wind turbine.



Table 1. Outline of previous studies. Re = Reynolds number; Exp.= experimental measurement; Num.= numerical simulation;

Author	Method	Re (x10)	Key features
Castelli et al.[10]	Num. 2D	5.2	Correlation between rotor power and torque concerning flow characteristics
Mohamed [31]	Num. 2D	N/A	Performance study of a turbine with different blade shapes
Mohamed [32]	Num. 2D	N/A	Aeroacoustic study on a three-bladed turbine
Rossetti and Paves [64]	Num. 2D and 3D	3.4	Start-up characteristics of turbine
Weber et al. [62]	Exp./Num.	2.8	Validation of numerical model with noise measurement of NACA0018 profile
Eboibi et al. [19]	Exp.	1.2-2.1	Performance study of a turbine concerning solidity effects
Howell et al. [9]	Exp.	0.67,1.00	Solidity effect and Surface roughness
Li et al. [13]	Exp.	0.8-1.1	Effect of blade's pitch angle, solidity and wind velocity
Du et al.[65]	Exp.	1.0, 0.81, 0.67	Effects of various design aspects concerning turbine start-up
Mazarbhuiya et al.[66]	Exp.	1.3-2.0	Effects of asymmetric blades with turbine performance
Desskosky et al. [63]	Num. 2D	2.8	Aerodynamic and Aeroacoustic study with a three-bladed rotor

III. METHODOLOGY

A. Computational domain and mesh details

The current study uses an unstructured mesh for the three-blade model. The computational domain consists of two areas, the stationary and the rotating regions (Figure 4). The overlapping grid method has been applied, permitting high-quality meshes specifically for every grid constituent. The rotor computational domain is circular with a radius R. The domain size in the x-direction is 24R (from -8R to 16R) and in the Y 16R (from 8R to -8R) (Figure 4). The receiver is situated at 1 m from the rotor centre to receive the acoustic signal (Figure 5). The grid system consists of 1.05 lakh cells with a near-wall distance $y^+ < 1$.

B. CFD settings

Aerodynamic Study: A comparison of published experimental findings and CFD for an H-rotor Darrieus turbine was used to evaluate the numerical turbulence model. When utilising the SST K- ω turbulence model, these results tell a good agreement between numerical and experimental functions of dB and Cp. Other investigations involving rotating blades and airfoils have shown a similar trend, demonstrating the SST K- ω use models for quick CFD calculations. For spinning bodies, the SST K- ω model is commonly preferred. A novel transport equation for the turbulent dissipation rate is included in this model. Compared to the standard k-model, the SST K- ω model usually produces better results for whirling and separation flows. Near all walls, the y^+ values are about one, within the required range for best-practice CFD. Depicts the torque coefficient variation for the rotor. After completing the first three revolutions, the statically stabilised state is reached. For the power curve computation, the last six revolutions are considered. A three-bladed NACA0021 profile with a chord length of 0.0858m and a Rotor radius of 0.515m makes up the Computational domain of the rotating region. The blades are joined with 0.25c spokes. The computational domain with blade profiles is shown in Figure.4. In this simulation, the spoke connection and shaft are disregarded to avoid unnecessary calculation time.

Aeroacoustic Study: The unsteady Reynolds averaged Navier Stokes (URANS) equations resolve the H-rotor Darrieus wind turbine's flow field. The noise emission is obtained using the Ffowcs Williams-Hawkings acoustic analogy using the "correlated length" method. The technique assumes that the vortex detaching correlates along a blade's firm length. The two-dimensional way can acquire major aerodynamic characteristics at a low cost. The rotating velocity of the airfoil is 83.78 rad/s. The finite volume method with the second-order upwind spatial discretisation scheme and second-order implicit temporal discretisation systems are used in the paper. The SIMPLE algorithm for pressure-velocity coupling and a fixed time-stepping (0.0001 s) method is adopted. The prior studies can establish the fluid-governing equations, correlation method, and the acoustic analogy. The CFD simulations were implemented in the ANSYS Fluent and developed a MATLAB code for acoustic signal treating. The NACA0018 airfoils are evenly distributed circumferentially in the flow field, and the link rod is not included in the study. The computational domain contains a rotating and stationary area. To characterise the blade aerodynamics and the relevant noise mechanisms, Weber experimented with the Reynolds number 28000. Hence, in this paper, the numerical analysis is carried out at Re 28000

C. Grid independence test

The total number of cells in the computational domain can influence the results due to the numerical approximations in RANS equations. However, the increase in grid size also necessitates more computational resources. Hence, a grid independence test is conducted in this paper to obtain a suitable mesh. Table 1 shows the grid independence tests with the acoustic parameter SPL_T (Eqn. 1), where SPL_T is the tonal SPL. The case-3 with 1.05 lakhs cells is selected in this paper. Beyond 1.05 lakhs, the acoustic property changes are found to be insignificant.

Table 1: Grid independence test

Case	No. of cells (Lakhs)	SPL _T (dB)
1	0.51	70.7
2	0.89	76.5
3	1.05	78.2
4	1.24	78.2

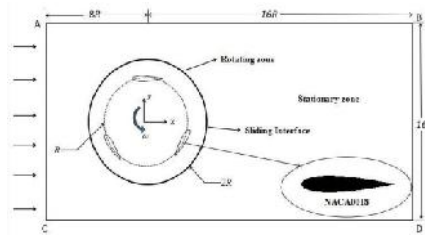


Figure. 4. Computational domain of three-bladed straight Darrieus wind turbine

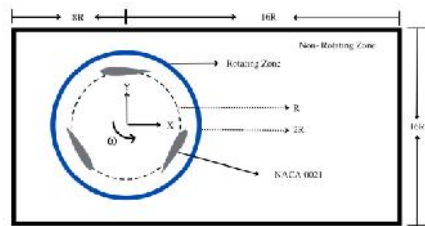


Figure.5. Computational domain of three-bladed straight Darrieus wind turbine

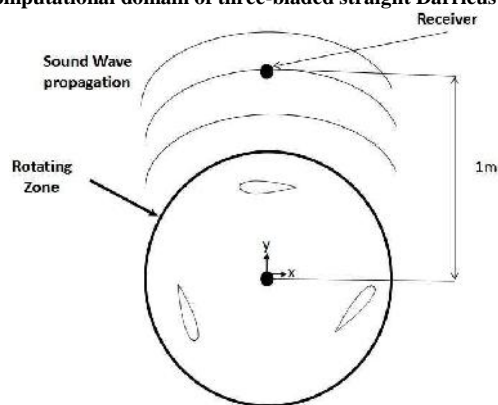


Figure.5.Receiver location

IV. RESULT AND DISCUSSION

A comparison of published experimental findings and CFD for an H-rotor Darrieus turbine was used to evaluate the numerical turbulence model. When utilising the SST K- turbulence model, these results tell a good agreement between numerical and experimental functions of dB and Cp. Other investigations involving rotating blades and airfoils have shown a similar trend, demonstrating the SST K- use models for quick CFD calculations. For spinning bodies, the SST K- model is commonly preferred. A novel transport equation for the turbulent dissipation rate is included in this model. Compared to the standard k- model, the SST K- model usually produces better results for whirling and separation flows. Near all walls, the y+ values are about one, within the required range for best-practice CFD. Depicts the torque coefficient variation for the rotor. After completing the first three revolutions, the statically stabilised state is reached. For the power curve computation, the last six revolutions are considered. The results show a good agreement between experimental and numerical results regarding prediction—validation of the experimental result in Table.5.



Table.2. Validation of the experimental result

Author	Method	Parameter	Validation	
			Author's result	Present study
Marco Raciti Castelli	Experimental	Power coefficient	0.3	0.272
Weber	Experimental	Overall sound pressure level(dB)	0.82	0.79

The turbine's self-noise depends on the blades' force variation and airflow through the spin. Thickness noise is continuously connected with loading sound, but not vice versa. Low Mac numbers generate only monotonous sound (thickness sound) and dipole sound (loading sound). However, sound pressure level is an important characteristic that indicates the sound an observer wants. Total sound emission depends on sound source power, spatial distribution, and temporal events. Radiation sound waves are superposed, displaying stout direction due to different radiations and phase offsets.

The Sound Pressure Level (SPL) is defined as,

$$SPL = 10 \log_{10} \left(\frac{f}{f_{pref}} \right)^2 \quad (1)$$

Where f is the frequency in Hz and $f_{pref} = 2 \times 10^{-5}$ Pa.

The noise output from the echo-free wind tunnel at the University of Erlangen-Nürnberg is measured at $Re=28000$ on a three-bladed H-rotor Darius wind turbine. The NACA0018 shape turbine's chord span is 0.05 m, and it has 0.4 m in diameter and 0.2 m tall. To measure acoustic pressure, free-field microphones were placed at a distance of 1 m. The blade passing frequency for the setup is 40Hz. Periodic signals observed for six complete revolutions of physical simulation time: 0.45 s. Figure 6 displays the numerically obtained SPL values with the experimental values. Acoustic results show the best fit in the critical frequency range. The blade passing frequency is the most vital regime, which is also accurately predicted. A significant peak can be seen at the blade passing frequency of 40 Hz. The comparison to the whole noise spectrum is made from 30 Hz because Weber reported that frequencies smaller than 30 Hz are wind tunnel noise.

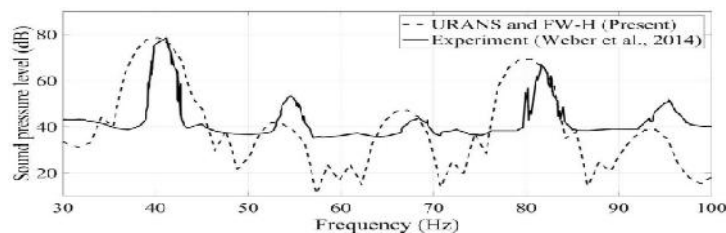


Figure.6. Numerical and Experimental comparison of the sound pressure level spectrum

A.Effects of Surface Roughness

It is possible to trip a boundary layer from laminar to turbulent flow with the right combination of surface roughness and Reynolds number, which increases skin friction drag. However, because a turbulent boundary layer is more resistant to separation from the rotor blade surface, the profile drag can be reduced where there was previously a separation with laminar flow. This could happen in such a way that, despite the increased skin drag, the overall drag on the aerofoil is minimised. Skin drag will be increased if the surface is too rough, and rapid variations in the surface profile will create locations for localised separation, increasing total drag. The blades' surface finish was visibly rough due to the manufacturing process. Because the blades were made of foam, it was impossible to utilise a surface profiler to identify the exact magnitude of the surface roughness. However, the enormous roughness scales were determined to be 0.3mm, 0.5mm, and 0.7mm in height, resulting in a non-dimensional roughness of (x/C) equal to 0.0001 to 0.0007. The turbine rotor blades were first put through their paces in their as-built state. The results were simulated in Fluent 19 and tabulated below. Table. 5, will explain the effect of surface roughness in power coefficient and sound pressure level. The effective surface roughness range lies between 0.0001 to 0.0003. Because further increasing surface roughness will improve the power coefficient and increase the level of sound.

TABLE Effect of Surface Roughness

Surface Roughness (Wall: Airfoil)	Power Coefficient (Cp)	Overall Sound Pressure level (dB)
0	0.272	93.6683
0.0001	0.2598	93.4931
0.0002	0.265676034	93.403
0.0003	0.281709	93.2098
0.0004	0.345873718	93.3816
0.0005	0.39	93.2694
0.0006	0.481133964	93.4691
0.0007	0.536282	93.3856

V. CONCLUSION

Darrieus VAWTs have the excellence of operating under small wind velocity and city zone circumstances. However, it writhes from deprived aerodynamic performance compared to HAWT. This paper's outcomes display the effect of using the H-rotor Darrieus VAWT on noise radiation. Numerical inquiries of an H-Darrieus wind turbine's noise production have been made to conform with the experimental data. There is a noble agreement among the numerical acoustic and experimental measurements. The examined operating point is characterised by the low tip-speed ratio of $\lambda = 0.4$ and $Re = 28000$. Using these CFD and CAA tools, aerodynamic and aeroacoustic optimisation can be accomplished concerning the design of VAWT. Forthcoming studies will include an emphasis on the acoustics of various pitch angles. The proposed method can be utilised for aeroacoustic optimisation to create VAWTs. The results clearly explain the effects of surface roughness; it is only effective on the below 0.0003 roughness range. Future investigations will emphasise the acoustics of various pitch angles incorporated with surface roughness. The proposed method can be used to improve the aeroacoustic performance of VAWTs.

ACKNOWLEDGEMENT

Authors wishing to acknowledge assistance or encouragement from colleagues, unique work by technical staff or financial support from organisations should do so in an unnumbered Acknowledgments section immediately following the last numbered section of the paper.

References

- [1] Du L, Ingram G, Dominy RG. A review of H-Darrieus wind turbine aerodynamic research. Proceedings of the Institution of Mechanical Engineers, Part C: Journal of Mechanical Engineering Science. 2019;233(23-24):7590-7616. doi:10.1177/0954406219885962
- [2] I. Hashem, M.H. Mohamed, Aerodynamic Performance Enhancements of H-rotor Darrieus Wind Turbine, Energy (2017), doi: 10.1016/j.energy.2017.10.036
- [3] Templin RJ. Aerodynamic performance theory for the NRC vertical-axis wind turbine. Laboratory technical report, LTR-LA-160, 1974. Ottawa: National Research Council of Canada.
- [4] Blackwell BF, Sheldahl RE and Feltz LV. Wind tunnel performance data for the Darrieus wind turbine with NACA0012 blades. SAND76-0130, 1977. Albuquerque,NM: Sandia Laboratories.
- [5] Consul CA, Willden RHJ, Ferrer E, et al. Influence of solidity on the performance of a cross-flow turbine. In: Proceedings of the 8th European wave and tidal energy conference, Uppsala, Sweden, January 2009.
- [6] Gosselin R, Dumas G and Boudreau M. Parametric study of H-Darrieus vertical-axis turbines using CFD simulations. Renew Sustain Energy 2016; 8.
- [7] Vassberg JC, Gopinath AK and Jameson A. Revisiting the vertical-axis wind turbine design using advanced computational fluid dynamics. In: The 43rd AIAA aerospace sciences meeting and exhibit, Reno, Nevada, USA, 10–13 January 2005.
- [8] Worstell MH. Aerodynamic performance of the 17-m-diameter Darrieus wind turbine in the three-bladed Configuration: an addendum. SAND-79-1753, 1982. Albuquerque, NM: Sandia Laboratories.
- [9] Howell R, Qin N, Edwards J, et al. Wind tunnel and numerical study of a small vertical axis wind turbine. Renew Energy 2010; 35: 412–422.
- [10] Castelli MR, Englaro A and Benini E. The Darrieus wind turbine: proposal for a new performance prediction model based on CFD. Energy 2011; 36: 4919–4934.
- [11] Subramanian A, Yogesh SA, Sivanandan H, et al. effect of airfoil and solidity on performance of small scale vertical axis wind turbine using three dimensional CFD model. Energy 2017; 133: 179–190.
- [12] Rezaeiha A, Montazeri H and Blocken B. Towards optimal aerodynamic design of vertical axis wind turbines: impact of solidity and number of blades. Energy 2018; 165: 1129–1148.
- [13] Li Q, Maeda T, Kamada Y, et al. effect of solidity on aerodynamic forces around straight-bladed vertical axis wind turbine by wind tunnel experiments (depending on number of blades). Renew Energy 2016; 96: 928–939.
- [14] Sagarichi A, Zamani M and Ghasemi A. Effect of solidity on the performance of variable-pitch vertical axis wind turbine. Energy 2018; 161: 753–775.
- [15] Kirke BK and Lazauskas L. Enhancing the performance of a vertical axis wind turbine using a simple variable pitch system. Wind Eng 1991; 15: 187–195.
- [16] Musgrove PJ and Mays ID. Development of the variable geometry vertical axis windmill. In: International symposium on wind energy systems, Amsterdam,Netherlands, 3–6 October 1978.
- [17] Roh SC and Kang SH. Effects of a blade profile, the Reynolds number, and the solidity on the performance of a straight bladed vertical axis wind turbine. J Mech Sci Technol 2013; 27: 3299–3307.
- [18] Simhan K. A review of calculation methods for the determination of performance characteristics of vertical axis wind energy converters with special reference to the influence of solidity and starting characteristics. Fachberichte Physik. Report no. 12, 1984. Bremen: Bremen University.
- [19] Eboibi O, Danao LAM and Howell RJ. Experimental investigation of the influence of solidity on the performance and flow field aerodynamics of vertical axis wind turbines at low Reynolds numbers. Renew Energy 2016;92: 474–483.
- [20] Singh MA, Biswas A and Misra RD. Investigation of self-starting and high rotor solidity on the performance of a three S1210 blade H-type Darrieus rotor. Renew Energy 2015; 76: 381–387
- [21] Sabaeifard P, Razzaghi H and Forouzandeh A. Determination of vertical axis wind turbines optimal configuration through CFD simulations. In: 2012 international conference on future environment and energy, Singapore, 2012.
- [22] Sabaeifard P, Razzaghi H and Forouzandeh A. Determination of vertical axis wind turbines optimal configuration through CFD simulations. In: 2012 international conference on future environment and energy, Singapore, 2012.
- [23] Berg DE. Customised airfoils and their impact on VAWT cost of energy. SAND90-1148C, 1990. Albuquerque,NM: Sandia Laboratories.
- [24] Klimas PC. Tailored airfoils for vertical axis wind turbines. SAND84-1062, 1992. Albuquerque, NM: Sandia Laboratories.
- [25] Masson C, Leclerc C and Paraschivoiu I. Appropriate dynamic-stall models for performance predictions of VAWTs with NLF blades. Int J Rotating Mach 1998;4: 129–139.
- [26] Angell RK, Musgrove PJ and Galbraith RAMcD. Unsteady wind tunnel testing of thick section aerofoils for use on large scale vertical axis wind turbine. In: Wind energy conversion, proceeding of 10th BWEA conference, London, UK, 22–24 March 1988, pp.195–203..
- [27] Islam M, Ting DSK and Fartaj A. Desirable airfoil features for smaller capacity straight bladed VAWT. Wind Eng 2007; 31: 165–196.
- [28] Bianchini A, Ferrari L and Magnani S. Start-up behavior of a three-bladed H-Darrieus vawt: experimental and numerical analysis. ASME Turbo Expo 2011; 6:811–820.
- [29] Bausas MD and Danao LAM. The aerodynamics of a camber-bladed vertical axis wind turbine in unsteady wind. Energy 2015; 93: 1155–1164.
- [30] Chen C-C and Kuo C-H. Effects of pitch angle and blade camber on flow characteristics and performance of small-size Darrieus VAWT. J Vis 2013; 16: 65–74.
- [31] Mohamed MH. Performance investigation of H-rotor Darrieus turbine with new airfoil shapes. Energy 2012;47: 522–530.
- [32] Mohamed MH. Aero-acoustics noise evaluation of H-rotor Darrieus wind turbines. Energy 2014; 65: 596–604.
- [33] Ma N, Lei H, Han Z, et al. Airfoil optimisation to improve power performance of a high-solidity vertical axis wind turbine at a moderate tip speed ratio. Energy 2018; 150: 236–252.

- [34] Migliore PG, Wolfe WP and Fanucci JB. Flow curvature effects on Darrieus turbine blade aerodynamics. *Energy* 1980; 4: 49–55.
- [35] Rainbird JM, Bianchini A, Balduzzi F, et al. On the influence of virtual camber effect on airfoil polars for use in simulations of Darrieus wind turbines. *Energy Convers Manag* 2015; 106: 373–384.
- [36] Sharpe DJ. Refinements and developments of the multiple streamtube theory for the aerodynamic performance of vertical axis wind turbines. In: *Proceedings of the BWEA wind energy conference*, 1984.
- [37] Paraschivoiu I and Delclaux F. Double-multiple streamtube model with recent improvements. *AIAA J* 1983; 7: 250–255.
- [38] [38] Paraschivoiu I, Frauni P and Beguier C. Streamtube expansion effects on the Darrieus wind turbine. *AIAA J* 1985; 1: 150–155.
- [39] Paraschivoiu I. Double-multiple streamtube model for studying vertical axis wind turbine. *AIAA J* 1987; 4:370–377.
- [40] Soraghan CE, Leithead WE, Feuchtwang J, et al. Double multiple streamtube model for variable pitch vertical axis wind turbines. In: *The 31st AIAA applied aerodynamics conference*, San Diego, USA, 24–27 June 2013.
- [41] Du L, Imgram G and Dominy RG. Time-accurate blade surface static pressure behaviour on a rotating HDarrieus wind turbine. *Wind Energy* 2019; 22: 563–575
- [42] Bossanyi EA. Wind turbine control for load reduction. *Wind Energy* 2003; 6: 229–244.
- [43] Kosaku T, Sano M and Nakatani K. Optimum pitch control for variable-pitch vertical-axis wind turbines by a single stage model on the momentum theory. In: *IEEE international conference on systems*, 2002.
- [44] Vandenberghe D and Dick E. Optimum pitch control for vertical axis wind turbines. *Wind Eng* 1987; 11: 237–247.
- [45] Chougule P and Nielsen S. Overview and design of selfacting pitch control mechanism for vertical axis wind turbine using multi body simulation approach. *J Phys Conf Ser* 2014; 524.
- [46] Chen B, Su S, Viola IM, et al. Numerical investigation of vertical-axis tidal turbines with sinusoidal pitching blades. *Ocean Eng* 2018; 155: 75–87.
- [47] Abdalrahman G, Melek W and Lien F. Pitch angle control for a small-scale Darrieus vertical axis wind turbine with straight blades (H-type VAWT). *Renew Energy* 2017; 114: 1353–1362.
- [48] Vandenberghe D and Dick E. A theoretical and experimental investigation into straight bladed vertical axis wind turbine with second order harmonic pitch control. *Wind Eng* 1987; 11: 237–247.
- [49] Bhutta M, Hayat N, Farooq AU, et al. Vertical axis wind turbine – a review of various configurations and design techniques. *Renew Sustain Energy Rev* 2012; 16: 1926–1939.
- [50] Rezaeiha A, Kalkman I and Blocken B. Effect of pitch angle on power performance and aerodynamics of a vertical axis wind turbine. *Appl Energy* 2017; 197: 132–150.
- [51] Parra-Santos T, Trullen DJP, Gallegos A, et al. Influence of fixed pitch angle on the performance of small scale. In: *Proceedings of the ASME 2016 fluids engineering division summer meeting*, Washington, DC, USA, 10–14 July 2016
- [52] Ashwill TD. Measured data for the Sandia 34 m vertical axis wind turbine. SAND91-2228, 1992. Albuquerque, NM: Sandia Laboratories.
- [53] Li Y, Tagawa K and Liu W. Performance effects of attachment on blade on a straight-bladed vertical axis wind turbine. *Curr Appl Phys* 2010; 10: S335–S338.
- [54] Prieuge L and Stoesser T. The influence of blade roughness on the performance of a vertical axis tidal turbine. *Int J Mar Energy* 2017; 17: 136–146.
- [55] Edwards JM. The influence of aerodynamic stall on the performance of vertical axis wind turbines. PhD Thesis, Sheffield University, UK, 2012.
- [56] Meana-Fernandez A, Solis-Gallego I, Oro JMF, et al. Parametrical evaluation of the aerodynamic performance of vertical axis wind turbines for the proposal of optimised designs. *Energy* 2018; 147: 504–517.
- [57] Armstrong S, Fiedler A and Tullis S. Flow separation on a high Reynolds number, high solidity vertical axis wind turbine with straight and canted blades and canted blades with fences. *Renew Energy* 2012; 41: 13–22.
- [58] Zanforlin S and Deluca S. Effects of the Reynolds number and the tip losses on the optimal aspect ratio of straight-bladed vertical axis wind turbines. *Energy* 2018; 148: 179–195.
- [59] Sheldahl RE, Klimas PC and Feltz LV. Aerodynamic performance of a 5-metre diameter Darrieus turbine with extruded NACA-0015 blades. SAND80-0179, 1980. Albuquerque, NM: Sandia Laboratories.
- [60] Danao LA, Eboibi O and Howell R. An experimental investigation into the influence of unsteady wind on the performance of a vertical axis wind turbine. *Appl Energy* 2014; 116: 111–124.
- [61] H. F. Lam, Y. M. Liu, H. Y. Peng, C. F. Lee, and H. J. Liu "Assessment of solidity effect on the power performance of H-rotor vertical axis wind turbines in turbulent flows" *Journal of Renewable and Sustainable Energy* 10, 023304 (2018); doi: 10.1063/1.5023120.
- [62] Weber J, Becker S, Scheit C, Grabinger J, Kaltenbacher M. Aeroacoustics of Darrieus Wind Turbine. *International Journal of Aeroacoustics*. 2015;14(5-6):883-902. doi:10.1260/1475-472X.14.5-6.883
- [63] Amgad Dessoky* , Galih Bangga, Thorsten Lutz, Ewald Kramer, "Aerodynamic and aeroacoustic performance assessment of H-rotor darrieus VAWT equipped with wind-lens technology" *Energy*, Volume 175, 15 May 2019, Pages 76-97.
- [64] Rossetti A and Pavesi G. Comparison of different numerical approaches to the study of the H-Darrieus turbines start-up. *Renew Energy* 2013; 50: 7–19.
- [65] Du L. Numerical and experimental investigations of Darrieus wind turbine start-up and operation. PhD Thesis, University of Durham, UK, 2016.
- [66] Mazarbhuiya H, Biswas A and Sharma KK. Performance investigations of modified asymmetric blade H-Darrieus VAWT rotors. *Renew Sustain Energy* 2018; 10.